

# Synthesis and Radiation Dosimetry of [<sup>68</sup>Ga]-Ga-Lys<sup>1</sup>, Lys<sup>3</sup>-DOTA-Bombesin (1,14) Antagonist for PET-Imaging, as a Potential Theragnostic Tracer in Oncology

Juan C. Manrique-Arias<sup>1,2\*</sup>, Quetzali Pitalua-Cortes<sup>1</sup>, Roberto Pedrero-Piedras<sup>1</sup>, Géiser Rodríguez-Mena<sup>1</sup>, Tessy López<sup>3</sup>, Cristian Cabezas-Ortiz<sup>1</sup>, Osvaldo García-Pérez<sup>1</sup>

<sup>1</sup>Departamento de Medicina Nuclear, Ciclotrón y Radiofarmacia Instituto Nacional de Cancerología, México City, México

<sup>2</sup>Cancer Center Cyclotron Department, Doctors Hospital, Monterrey, México

<sup>3</sup>Departamento de Atención a la Salud, Universidad Autónoma Metropolitana-Xochimilco, México City, México

Email: \*juancmanriquea@unam.mx

**How to cite this paper:** Manrique-Arias, J.C., Pitalua-Cortes, Q., Pedrero-Piedras, R., Rodríguez-Mena, G., López, T., Cabezas-Ortiz, C. and García-Pérez, O. (2020) Synthesis and Radiation Dosimetry of [<sup>68</sup>Ga]-Ga-Lys<sup>1</sup>, Lys<sup>3</sup>-DOTA-Bombesin (1,14) Antagonist for PET-Imaging, as a Potential Theragnostic Tracer in Oncology. *Journal of Encapsulation and Adsorption Sciences*, 10, 29-41.

<https://doi.org/10.4236/jeas.2020.102002>

**Received:** May 22, 2020

**Accepted:** June 19, 2020

**Published:** June 22, 2020

Copyright © 2020 by author(s) and Scientific Research Publishing Inc.

This work is licensed under the Creative Commons Attribution International License (CC BY 4.0).

<http://creativecommons.org/licenses/by/4.0/>



Open Access

## Abstract

This Bombesin (BBN), a tetradecapeptide analog of human gastrin-releasing peptide (GRP) with a high binding affinity for GRP receptors (GRPR), is over-expressed in early stages of androgen-dependent prostate carcinomas, but not in advanced stages. Therefore, there is a need to develop effective tracers for the accurate and specific detection of this disease. The objective of this study was to evaluate Lys<sup>1</sup>, Lys<sup>3</sup>-DOTA-BBN (1,14) analog with the radiolabeled positron emitter [<sup>68</sup>Ga]-Ga-BBN for receptor imaging with PET, and to determine its biodistribution and radiation dosimetry using whole-body (WB) PET scans in healthy volunteers. The highest uptake was in the pancreas, followed by urinary bladder. The critical organ was pancreas with a mean absorbed dose of 206 ± 0.7, 210 ± 0.7, 120 ± 0.9, 390.23 ± 0.6 μGy/MBq and the effective doses were estimated as 73.2 ± 0.6, 49.8 ± 0.3 μGy/MBq (women and men, respectively).

## Keywords

Radiation Dosimetry, Biodistribution, PET Imaging, Radiopharmaceutical, Lys<sup>1</sup>, Lys<sup>3</sup>-DOTA-BBN (1,14), Bombesin Analogs

## 1. Introduction

In 2018, 9.5 million deaths due to cancer were reported (excluding non-melanoma skin cancer), and of these, lung cancer was the most frequent in both sexes, with

a mortality rate of 11.6%, thus becoming the leading cause of death, followed by breast, colorectal, stomach, liver, and prostate cancer.

Prostate cancer (PCa) accounts for 29% of all tumors, and it is the second most common cause of cancer-related deaths in men globally. There is an urgent need for improving imaging techniques that will provide accurate staging and monitoring of this disease, particularly at the early stages. There are conventional imaging techniques which have limited sensitivity and specificity for detecting primary metastatic and recurrent PCa, such as ultrasound, contrast-enhanced CT or MR [1] [2].

$^{68}\text{Ga}$ -labeled peptides have become relevant for diagnostic imaging due to their favorable pharmacokinetics as a radiotracer for positron emission tomography (PET). Gastrin releasing peptide receptor (GRPR), also known as bombesin (BBN) receptor subtype II, is part of the group G protein-coupled receptor family of bombesin, and it has been reported to be useful in various types of cancer, including breast, prostate, colorectal, pancreatic, glioma, lung and gastrointestinal stromal cancers [3].

GRPR has become an interesting target for receptor-mediated tumor imaging and treatment. It is also known that BBN antagonists are not internalized, whereas radiopharmaceuticals based on Lys<sup>1</sup> Lys<sup>3</sup>-Bombesin (BBN agonists) have a significant internalization rate [4]. It has also been reported that the DOTA chelator is responsible for the low internalization of the radioligands based on PSMA inhibitors [5] [6], and its intermediate position between two peptide chains could induce a steric shielding effect on DOTA that decreases its biological interaction.

Some recent reports have shown that GRPR antagonists are preferable to GRPR agonists, allowing for a greater tumor uptake compared to non-target tissue and lower side effects due to the drug [7]. Good progress has been reported for the GRPR antagonist for PET imaging and radionuclide therapy of PCa [8] [9]. The main objective of this study was to estimate the human radiation dosimetry of [ $^{68}\text{Ga}$ ]-Ga -Lys<sup>1</sup>, Lys<sup>3</sup>-DOTA-BBN analog, using the biodistribution information obtained from serial WB PET/CT scans in healthy human subjects after administration the radiopharmaceutical.

## 2. Experimental

### 2.1. General

Peptide conjugate was obtained at the Instituto Nacional de Investigaciones Nucleares (ININ-México) and purchased from piChem laboratory (Graz, Austria) packaged at 1 mg per vial, K-Q-K(DOTA)-L-G-N W-A-V--G-H-L-M-NH<sub>2</sub> (Lys<sup>1</sup>, Lys<sup>3</sup>-DOTA-BBN (1,14)) **Figure 1**, ultrapure hydrochloric acid 30% and sodium acetate were acquired from Sigma-Aldrich (St. Louis, MO, USA), C18 light cartridges were obtained from Waters (Milford, Massachusetts, USA), 0.22  $\mu\text{m}$  pore size syringe filters were from Millipore. All radioactivity measurements were done with Capintec CRC<sup>®</sup> 25 PET dose calibrator in  $^{68}\text{Ga}$ -window mode.

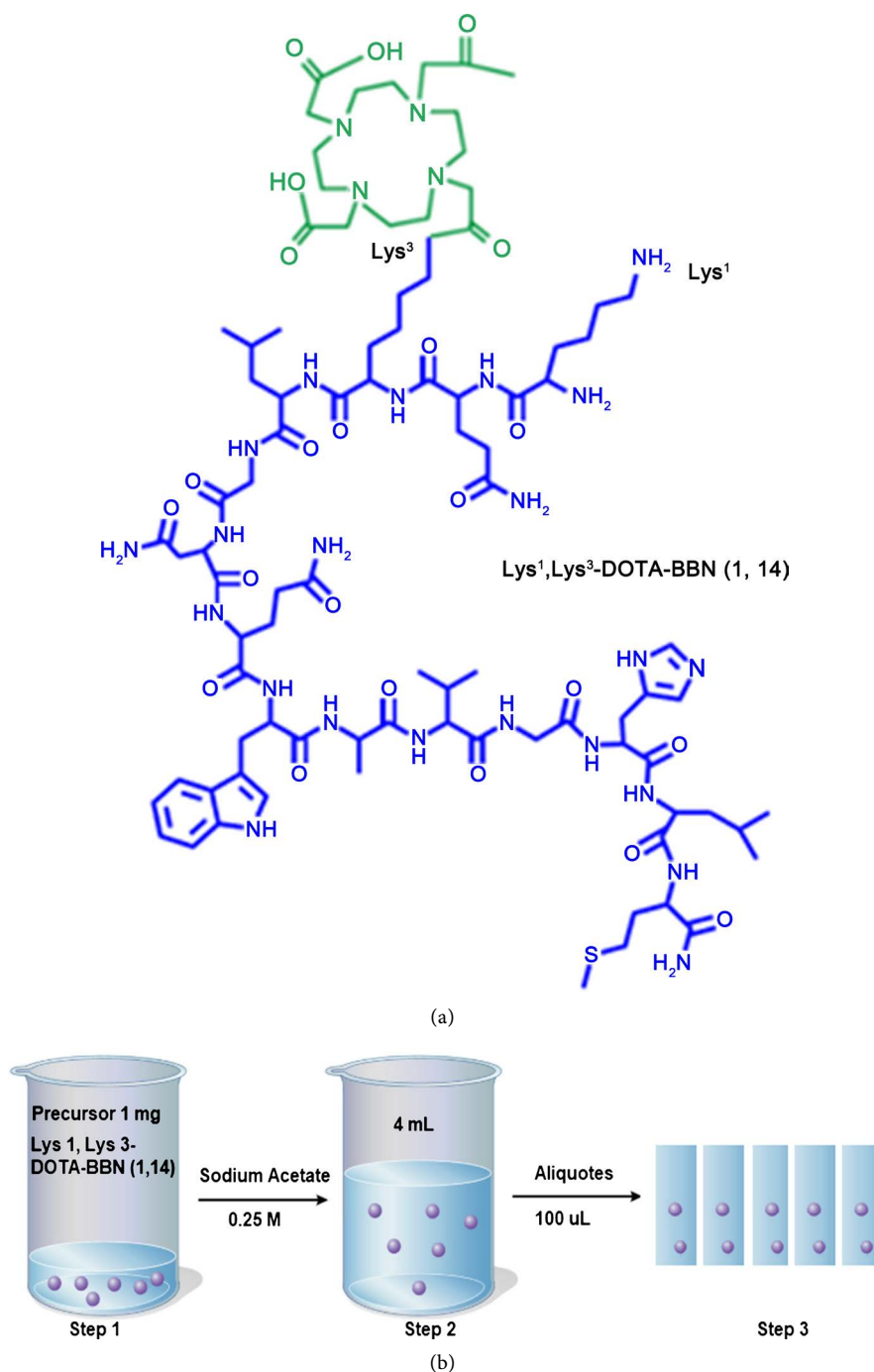


**Figure 1.** (a) Structure of Lys<sup>1</sup>, Lys<sup>3</sup>-DOTA-BBN (1,14); (b) Preparation diagram of Lys<sup>1</sup> Lys<sup>3</sup>-DOTA-BBN (1,14).

## 2.2. Labeling of Lys<sup>1</sup> Lys<sup>3</sup>-DOTA-BBN (1,14) with <sup>68</sup>Ga

A stock solution of precursor Lys<sup>1</sup> Lys<sup>3</sup>-DOTA-BBN (1,14), was prepared by dissolving 1 mg in 0.25 M Sodium acetate solution; aliquots of 100 µl (25 µg) of this stock solution were dispensed in 1 mL Eppendorf tubes, and stored at -20°C **Figure 1(a)**.

Gallium was obtained in a commercial ITG <sup>68</sup>Ge/<sup>68</sup>Ga generator (Isotope Tech-

nologies Garching GmbH, Germany) and eluted directly to the reaction vessel containing 25 µg of peptide previously dissolved with 1 mL of 0.25 M NaOAc. The mixture was heated for 5 minutes at 105 °C and then incubated for 12 min, using the IQS Ga-68 Fluidic labeling module. All the production processes and quality control (QC) procedures were validated to be in compliance with GMP [10].

### 2.3. Purification

Purification of the radioligand was made with a Sep Pak C18 Light cartridge and the product eluted with 1 mL of 70% EtOH. The final product was diluted with 5 mL of 0.9% NaCl and sterilized by filtration using a 0.22 µm, Millex-GV filter.

### 2.4. Quality Control

The radiochemical purity (RCP) of the labeled compound was determined by analytical HPLC provided with UV and radiation detectors. The analysis was performed using a Nova-Pak C8 column (3.9 × 150 mm) with a flow rate of 2 ml/min. Eluent components were A = 0.1 N TFA (trifluoroacetic acid) and B = CH<sub>3</sub>CN (acetonitrile) and the following gradient elution technique was adopted for separation: 0 - 1.5 min 95% A + 5% B isocratic, 1.5 - 2.0 min from 5% to 100% B in linear-gradient, 2 - 3 min 100% B, 3 - 4 min from 100% to 5% B in linear gradient.

### 2.5. Stability in Human Serum

The stability of <sup>68</sup>Ga-Lys<sup>1</sup>, Lys<sup>3</sup>-DOTA-BBN (1,14) was determined in serum. Aliquot of 200 µl of the radiopharmaceutical was diluted (1:10) with fresh human serum and incubated at 37 °C. The radiochemical stability was determined in 100 µL samples taken at different times from 30 to 180 minutes and analyzed by thin-layer chromatography in TLC-SG using methanol as the mobile phase.

### 2.6. Human Subjects

Twelve healthy volunteers were included (6 women and 6 men; mean age ± SD, 50 ± 12 years; age range, 37 - 70 years; mean weight ± SD, 75 ± 2 kg; weight range, 66 - 94 kg). Volunteers were recruited at the Instituto Nacional de Cancerología. The study was conducted in accordance with the Declaration of Helsinki with the Ethics Committee approval (Rev/78/17). Each subject signed written informed consent for entering the study.

### 2.7. PET/CT

All patients underwent [<sup>68</sup>Ga] Ga-Lys<sup>1</sup>, Lys<sup>3</sup>-DOTA-BBN (1,14) PET/CT using an mCT Excel 20 PET/CT scanner (Siemens, Erlangen, Germany) consisting of a bismuth orthosilicate full scanner and a 20-detector-row CT scanner. Whole-body CT was performed before the injection of 190 ± 28 MBq of [<sup>68</sup>Ga]-Ga-Lys<sup>1</sup>, Lys<sup>3</sup>-DOTA-BBN, and transmission data were acquired using low-dose CT (120

kV, automated from 100 - 130 mA, a  $512 \times 512$  matrix, a 50-cm field of view (FOV), 3.75-mm slice thickness, and a rotation time of 0.8 s), extending from the base of the skull to the proximal thighs. At 1, 10, 30, 60 and 90 minutes after tracer injection, a whole-body PET was acquired in 3D (matrix  $168 \times 168$ ). For each bed position (16.2 cm, overlapping scale 4.2 cm), we used a 2-min acquisition time with a 15.5-cm field of view (FOV). The emission data were corrected for randoms, scatter and decay. Reconstruction was conducted with an ordered subset expectation maximization (OSEM) algorithm with 3 iterations/12 subsets and Gauss-filtered to a transaxial resolution of 5 mm at full-width at half-maximum (FWHM). Attenuation correction was performed using low-dose non-enhanced CT.

The PET/CT images were transferred to a multimodal workstation (Syngo TrueX and HD Truepoint Siemens Medical Solution) for data analysis. Regions of interest (ROIs) were outlined over the major organs based on the contour of CT images.

## 2.8. Dosimetry

In this study, the absorbed radiation and the effective doses were calculated based on the RADAR method [11] by entering the time-integrated activity coefficient of each source organ onto OLINDA/EXM 1.1 software (Organ Level Internal Dose Assessment Code, Vanderbilt University, Nashville, USA) using the reference adult male and female models [12].

The quantification of images is comparable to the methodology and principles of the MIRD 16 document [13].

The residence time of urine in the bladder was calculated by the Prism model and the time-integrated activity coefficients for the gastrointestinal tract were estimated using the ICPR 30 gastrointestinal (GI) tract model [14]. The remaining activity in the body was calculated for each time point as the value resulting from the original activity injected, minus the activity left in the organs. The effective dose was calculated by entering the time-integrated activity coefficient for the source organs into OLINDA/EXM.

## 2.9. Statistical Analysis

Statistical analysis was performed by GraphPad Prism software (version 5.01) and the results are expressed at a precision of 1 SD (mean  $\pm$  SD).

# 3. Results

## 3.1. Synthesis and Radiochemistry

After SPE cartridge purification, the final product ( $[^{68}\text{Ga}]\text{-Ga-BBN}$ ) was obtained with a radiochemical yield of  $65\% \pm 4\%$  ( $n > 10$ ) and a radiochemical purity (RCP)  $> 93\%$ . The average specific activity of the purified product was determined to be  $47.2 \pm 7.2$  GB/ $\mu\text{mol}$ . The retention time for  $^{68}\text{Ga}$ -free was  $0.5 \pm 0.02$  min, while the retention time for  $^{68}\text{Ga-BBN}$  was 2.79 minutes (**Figure 2**).

### 3.2. Stability Test in Human Serum

The binding of the [ $^{68}\text{Ga}$ ]-Ga-Lys<sup>1</sup>-Lys<sup>3</sup>-DOTA-BBN (1,14) to the serum proteins and its *in-vitro* metabolism was assessed by incubating the compound in fresh human serum for 3 h at 37°C. At selected time-intervals, 10  $\mu\text{l}$  aliquots were tested for [ $^{68}\text{Ga}$ ]-Ga-Lys<sup>1</sup>-Lys<sup>3</sup>-DOTA-BBN, the instability product, detected by thin-layer chromatography on TLC-SG using methanol as the mobile phase. [ $^{68}\text{Ga}$ ]-Ga-Lys<sup>1</sup>-Lys<sup>3</sup>-DOTA-BBN (1,14) was stable with only about 2% free  $^{68}\text{Ga}$  detected after almost 3 h (Figure 3).

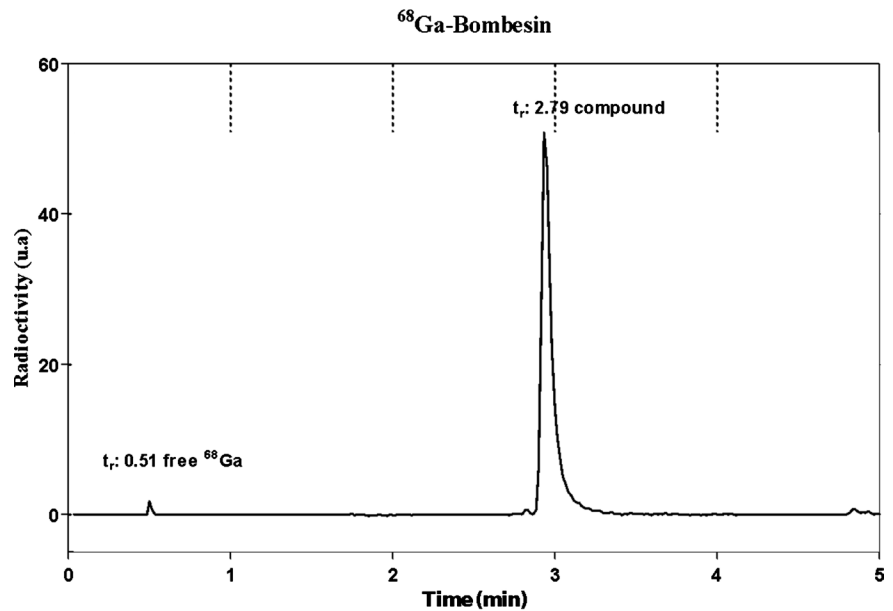


**Figure 2.** Radio HPLC profile of the [ $^{68}\text{Ga}$ ]-Ga-Lys<sup>1</sup>, Lys<sup>3</sup>-DOTA-BBN (1,14), labeled peptide has a retention time of 2.79 and free  $^{68}\text{Ga}$  retention time of 0.51 minutes, respectively.

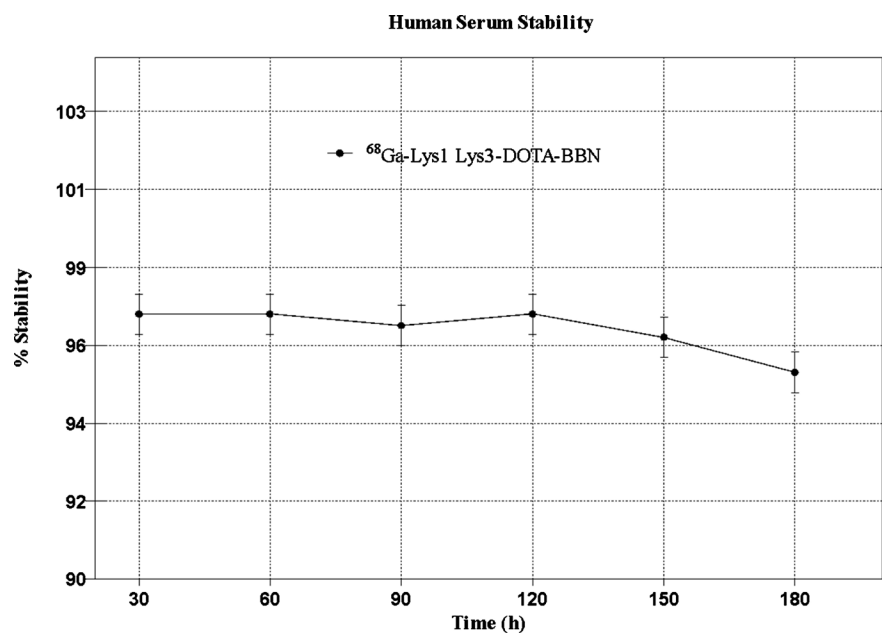


**Figure 3.** Stability of [ $^{68}\text{Ga}$ ]-GaLys<sup>1</sup>-Lys<sup>3</sup>-DOTA-BBN (1,14) in human serum (n = 3).

### 3.3. Biodistribution and Dosimetry

After intravenous administration of  $190 \pm 28$  MBq of [ $^{68}\text{Ga}$ ]-Lys<sup>1</sup>, Lys<sup>3</sup>-DOTA-BBN (1,14), the compound showed rapid accumulation through the pancreas with  $37.6\% \pm 4.3\%$  of the total injected radioactivity found in the urine at 10 min post-injection. **Figure 4** shows the normal biodistribution of the radiopharmaceutical at different times post-injection. The biodistribution data (%ID/organ), are shown in **Figure 5** for the kidneys, pancreas, urinary bladder. We can observe in **Table 1** the amounts of radio-activity vs time for the different organs.

### 4. Discussion

The tracer radioactivity was accumulated predominantly in the pancreas, urinary bladder, and kidneys. The dosimetry results indicate that the critical organ is the pancreas, followed by the urinary bladder where the absorbed doses reached  $206 \pm 0.7$ ,  $210 \pm 0.7$ ,  $120 \pm 0.9$ ,  $390.23 \pm 0.6$   $\mu\text{Gy}/\text{MBq}$  and the effective doses were estimated as  $73.2 \pm 0.6$ ,  $49.8 \pm 0.3$   $\mu\text{Gy}/\text{MBq}$  (women and men, respectively). **Table 1** shows the absorbed dose of the different organs.

Currently, the use of radiolabeled GRPR antagonists for targeting tumors *in vivo* has gained much attention, with somatostatin receptor antagonists showing higher tumor uptake and targeting more receptor-binding sites than their agonist

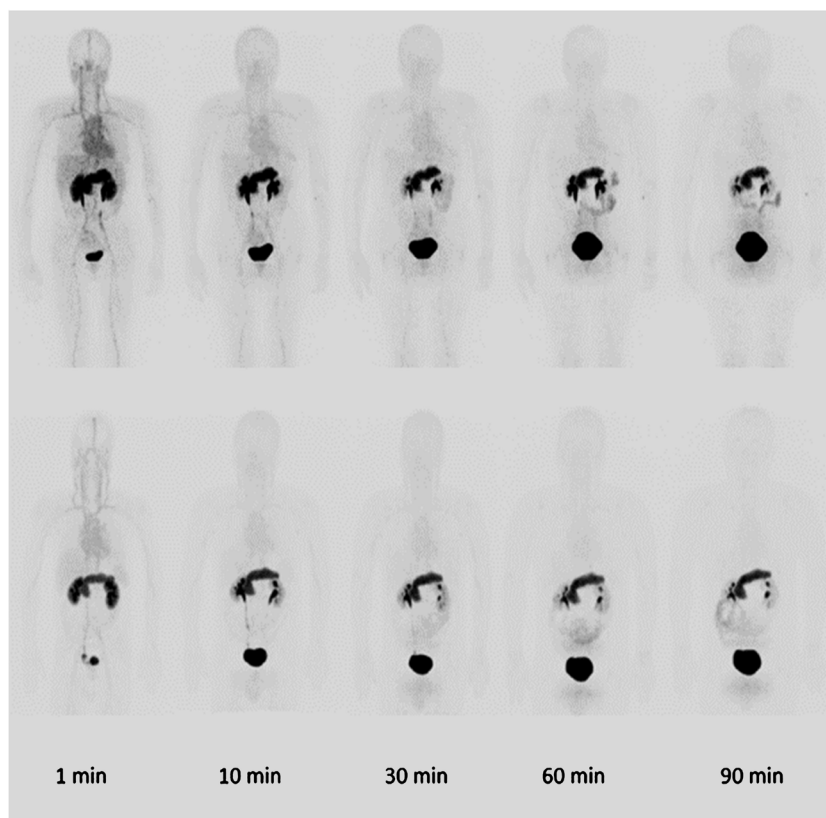


**Figure 4.** Whole-body PET images of the biodistribution of [ $^{68}\text{Ga}$ ]-GaLys<sup>1</sup>-Lys<sup>3</sup>-DOTA-BBN (1,14) at 1, 10, 30, 60, and 90 minutes after intravenous administration to female (top row) and male (bottom row) patients.



[15] [16] [17]. The use of these radiolabeled somatostatin receptors with Gallium-68 for imaging and diagnosis of neuroendocrine tumors has stimulated research in the detection of other receptors of additional tumor types [18], not only for diagnosis but also for therapy.

These receptors can be overexpressed in different types of human tumors such as breast and prostate cancer [19] [20] [21]. Controversy persists in the use of agonists vs. GRPR antagonists; however, several studies have shown the superiority of

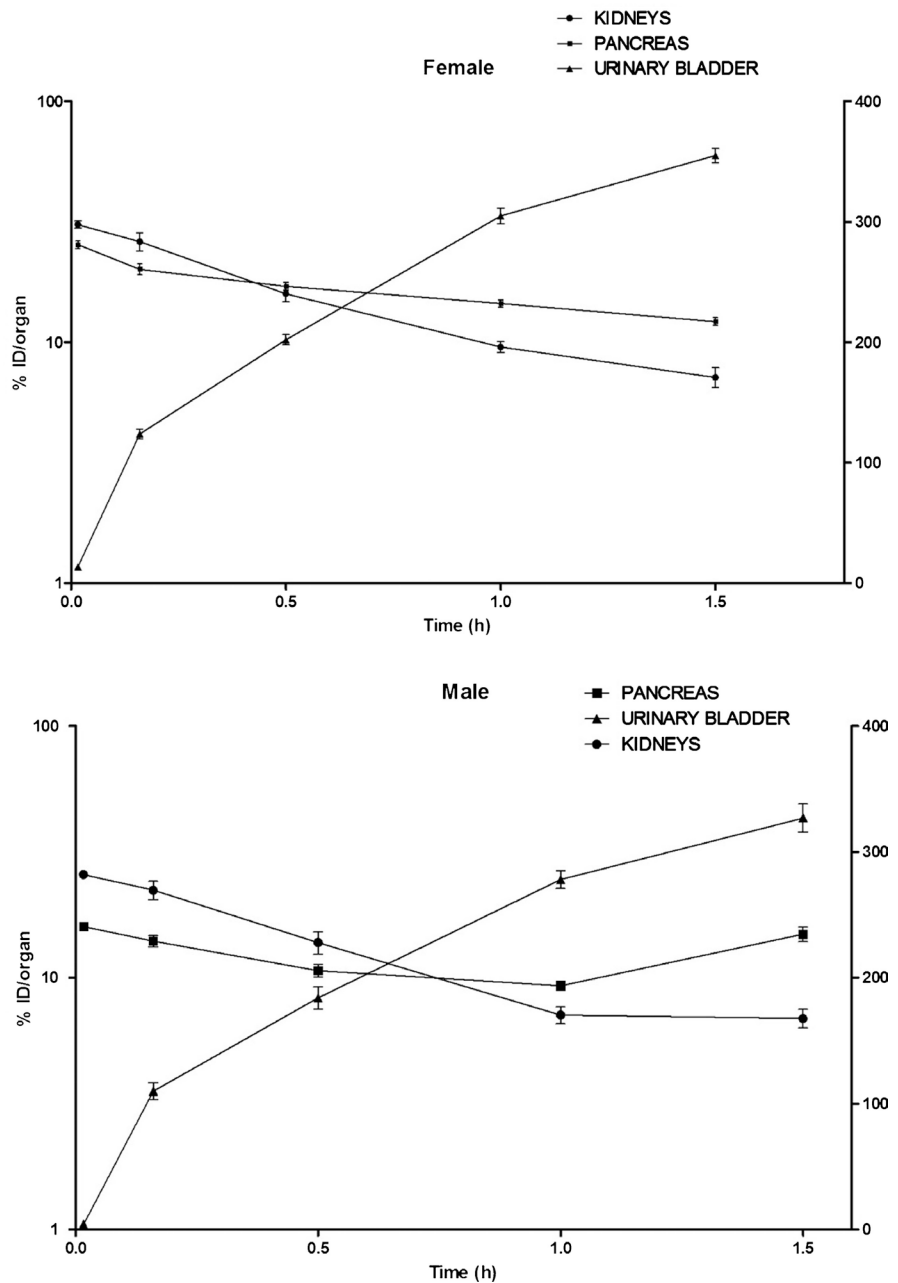


**Figure 5.** Decay corrected averaged time-activity curves  $[^{68}\text{Ga}]\text{-Ga-Lys}^1\text{-Lys}^3\text{-DOTA-BBN}$  (1,14) in the pancreas, urinary bladder and kidneys for all healthy volunteers. The time-integrated activity coefficients for various organs in men and women are listed in **Table 1**.



**Table 1.** Estimated Absorbed dose after administration of [<sup>68</sup>Ga]-GaLys<sup>1</sup>-Lys<sup>3</sup>-DOTA-BBN (1,14) in healthy subjects (MEAN ± SD).

Organ	Adult Female Absorbed Dose (μGy/MBq)	Adult Male Absorbed Dose (μGy/MBq)
Adrenals	10.30 ± 0.7	8.37 ± 0.8
Brain	7.16 ± 0.7	5.71 ± 0.7
Breasts	7.16 ± 0.7	5.67 ± 0.7
Gallbladder Wall	10.40 ± 0.6	8.49 ± 0.9
Lli Wall	21.20 ± 0.7	15.60 ± 1.5
Small Intestine	13.60 ± 0.4	10.30 ± 0.9
Stomach Wall	10.20 ± 0.6	8.37 ± 1.0
Uli Wall	12.60 ± 0.5	9.48 ± 0.8
Heart Wall	8.61 ± 0.8	6.90 ± 0.8
Kidneys	58.60 ± 0.5	54.50 ± 0.7
Liver	9.04 ± 0.7	7.24 ± 0.8
Lung	8.03 ± 0.7	6.48 ± 0.9
Muscle	10.70 ± 0.5	8.42 ± 0.8
Ovaries	20.60 ± 0.7	-----
Pancreas	206.00 ± 0.7	210.00 ± 0.7
Red Marrow	8.47 ± 0.4	6.72 ± 0.6
Osteogenic Cells	13.00 ± 0.7	9.66 ± 1.1
Skin	7.81 ± 0.6	6.23 ± 0.6
Spleen	10.40 ± 0.7	8.49 ± 0.9
Testes	--	12.00 ± 0.1
Thymus	7.91 ± 0.8	6.27 ± 0.7
Thyroid	7.41 ± 0.8	6.17 ± 0.7
UrinaryBladder Wall	120.00 ± 0.9	390.23 ± 0.6
Uterus	33.60 ± 0.8	-----
Total Body	11.60 ± 0.5	9.02 ± 0.8
Effective Dose (μSv/MBq)	73.20 ± 0.6	49.80 ± 0.3

the antagonists, with a higher degree of uptake of the radiotracer in tumors, especially when studying prostate cancer [22] [23] [24] (Figure 6).

Data on bio-distribution (%ID/g) of [<sup>68</sup>Ga]-Ga-Lys<sup>1</sup>, Lys<sup>3</sup>-DOTA-BBN (1,14) in healthy volunteers show its predominant uptake in the pancreas, urinary bladder, and kidneys which suggests high metabolic activity of gallium in these organs. No uptake in the brain was observed and elimination by urine was predominant.

The dosimetry calculations revealed the pancreas as the critical organ with a mean absorbed doses of 206 ± 0.7 and 210 ± 0.7 μGy/MBq (women and men,

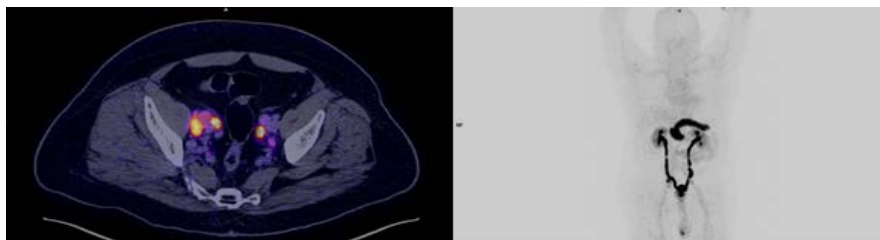


**Figure 6.** 67 years old male patient with biochemical relapse prostate cancer.  $^{68}\text{Ga}$ -Lys<sup>1</sup>-Lys<sup>3</sup>-DOTA-BBN PET/CT shows increased uptake in pelvic lymph nodes.

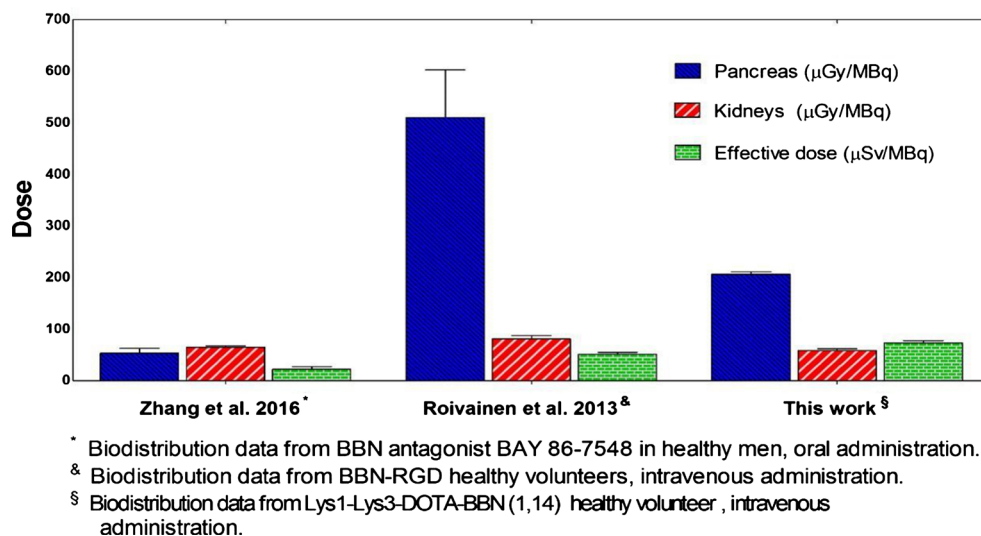


**Figure 7.** Estimates of the absorbed radiation doses to the specified human critical organs, pancreas, kidneys and the effective doses after administrations of [ $^{68}\text{Ga}$ ]-Ga-Lys<sup>1</sup>, Lys<sup>3</sup>-DOTA-BBN (1,14) were reported in this research and in the previous publications.

respectively). Moreover, the mean WB effective dose was  $61.5 \pm 0.5 \mu\text{Gy/MBq}$ .

It should be noted in general that the radiation dose is higher for females than males. This is a result of the smaller body and organ sizes. In addition, the female gonads receive a higher dose of radiation, as well as the liver and kidneys due to the closeness to these organs.

**Figure 7** summarizes the estimated absorbed dose from [ $^{68}\text{Ga}$ ]-Ga-Lys<sup>1</sup>, Lys<sup>3</sup>-DOTA-BBN in humans obtained in this work. The results shown in this Figure can be compared directly with other studies because the biodistribution data were obtained under similar conditions. Our effective doses seem to be in reasonable agreement with others [25] [26]. The differences in the results show the discrepancies among the metabolic activities of the subjects studied.

Considering the kinetics of the radiotracer, the acquisition of diagnostic images is suggested to be between 60 - 90 minutes post-injection, after this time a smaller amount of recirculating radio-tracer is observed so that the tumor-to-background ratio is better [27].

## 5. Conclusion

In conclusion [ $^{68}\text{Ga}$ ]-Ga-Lys<sup>1</sup>, Lys<sup>3</sup>-DOTA-BBN (1,14) is a promising PET radi-

otracer for the early detection and prognosis of prostate tumors with a favorable biodistribution, fast clearance, low immunogenicity, and a good dosimetry profile. The feasibility and advantage of using radiolabeled bombesin peptides as agents for the identification of tumors that overexpress gastrin-releasing peptide receptors is possible with multiple radioisotopes such as  $^{99m}\text{Tc}$ ,  $^{68}\text{Ga}$ ,  $^{64}\text{Cu}$ ,  $^{177}\text{Lu}$ ,  $^{111}\text{In}$ ,  $^{18}\text{F}$  and  $^{86}\text{Y}$ , many of these with characteristics that allow therapeutic uses. In all cases, the results show the pancreas as the critical organ with a mean absorbed doses of  $206 \pm 0.7$  and  $210 \pm 0.7$   $\mu\text{Gy}/\text{MBq}$  (women and men, respectively), and the mean WB effective dose as  $61.5 \pm 0.5\mu\text{Gy}/\text{MBq}$ .

### Acknowledgements

This study was supported by Unidad Ciclotrón Radiofarmacia Instituto Nacional de Cancerología. We are grateful to Dr. G Ferro-Flores Instituto Nacional de Investigaciones Nucleares, for providing the peptide to carry out this research. MSc Victoria López Rodríguez and Carmen Dence contributed to the study design and manuscript editing and review.

### Ethical Approval

This study was conducted in accordance with the Declaration of Helsinki with the Ethics Committee approval (Rev/78/17) of the National Institute of Cancerology. Each subject signed written informed consent for entering the study.

### Conflicts of Interest

The authors declare no conflicts of interest regarding the publication of this paper.

### References

- [1] Malik, A.S., Boyko, O., Atkar, N. and Young, W.F. (2001) A Comparative Study of MR Imaging Profile of Titanium Pedicle Screws. *Acta Radiologica*, **42**, 291-293. <https://doi.org/10.1080/028418501127346846>
- [2] Ferlay, J., Shin, H.R., Bray, F., Forman, D., Mathers, C. and Parkin, D.M. (2010) Estimates of Worldwide Burden of Cancer in 2008: GLOBOCAN 2008. *International Journal of Cancer*, **127**, 2893-2917. <https://doi.org/10.1002/ijc.25516>
- [3] Bray, F., Ferlay, J., Soerjomataram, I., Siegel, R.L., Torre, L.A. and Jemal, A. (2018). Global Cancer Statistics 2018: GLOBOCAN Estimates of Incidence and Mortality Worldwide for 36 Cancers in 185 Countries. *CA: A Cancer Journal for Clinicians*, **68**, 394-424. <https://doi.org/10.3322/caac.21492>
- [4] Cescato, R., Maina, T., Nock, B., *et al.* (2008) Bombesin Receptor Antagonist May Be Preferable to Agonist for Tumor Targeting. *Journal of Nuclear Medicine*, **49**, 318-326. <https://doi.org/10.2967/jnumed.107.045054>
- [5] Ferro-Flores, G., de Murphy, C.A., Rodríguez-Cortés, J., *et al.* (2006) Preparation and Evaluation of  $^{99m}\text{Tc}$ -EDDA/HYNIC-[Lys<sup>3</sup>]-Bombesin for Imaging Gastrin-Releasing Peptide Receptor-Positive Tumours. *Nuclear Medicine Communications*, **27**, 371-376. <https://doi.org/10.1097/01.mnm.0000202863.52046.7f>
- [6] Wu 'stemann, T., Bauder-Wu 'st, U., Scha 'fer, M., *et al.* (2016) Design of Internaliz-

- ing PSMA-Specific Gluureido-Based Radiotherapeutics. *Theranostics*, **6**, 1085-1095. <https://doi.org/10.7150/thno.13448>
- [7] Ray Banerjee, S., Chen, Z., Pullambhatla, M., *et al.* (2016) Preclinical Comparative Study of  $^{68}\text{Ga}$ -Labeled DOTA, NOTA, and HBED-CC Chelated Radiotracers for Targeting PSMA. *Bioconjugate Chemistry*, **27**, 1447-1455. <https://doi.org/10.1021/acs.bioconjchem.5b00679>
- [8] Saatchi, K., Gelder, N., Gershkovich, P., Sivak, O., Wasan, K.M., Kainthan, R.K., Brooks, D.E. and Häfeli U.O. (2012) Long-Circulating Non-Toxic Blood Pool Imaging Agent Based on Hyperbranched Polyglycerols. *International Journal of Pharmaceutics*, **422**, 418-427. <https://doi.org/10.1016/j.ijpharm.2011.10.036>
- [9] Reubi, J.C., Körner, M., Waser, B., Mazzucchelli, L. and Guillou, L. (2004) High Expression of Peptide Receptors as a Novel Target in Gastrointestinal Stromal Tumours. *European Journal of Nuclear Medicine and Molecular Imaging*, **31**, 803-810.
- [10] Yang, M., Gao, H., Zhou, Y., *et al.* (2011)  $^{18}\text{F}$ -Labeled GRPR Agonists and Antagonists: A Comparative Study in Prostate Cancer Imaging. *Theranostics*, **1**, 220-229. <https://doi.org/10.7150/thno/v01p0220>
- [11] Alejandro, A.C., Megan, S., Marian, M., Shankar, V. and John W., B. (2016) Comprehensive Quality Control of the ITG  $^{68}\text{Ge}/^{68}\text{Ga}$  Generator and Synthesis of  $^{68}\text{Ga}$ -DOTATOC and  $^{68}\text{Ga}$ -PSMA-HBED-CC for Clinical Imaging. *The Journal Nuclear Medicine*, **57**, 1402-1405. <https://doi.org/10.2967/jnumed.115.171249>
- [12] Stabin, M.G. and Siegel, J.A. (2003) Physical Models and Dose Factor for Use in Internal Dose Assessment. *Health Physics*, **85**, 294-310. <https://doi.org/10.1097/00004032-200309000-00006>
- [13] Stabin, M.G., Sparks, R.B. and Crowe, E. (2005) OLINDA/EXM: The Second-Generation Personal Computer Software for Internal Dose Assessment in Nuclear Medicine. *Journal of Nuclear Medicine*, **46**, 1023-1027.
- [14] Siegel, J.A., Thomas, S.R., Stubbs, J.B., *et al.* (1999) MIRD Pamphlet No. 16: Techniques for Quantitative Radiopharmaceutical Biodistribution Data Acquisition and Analysis for Use in Human Radiation Dose Estimates. *Journal of Nuclear Medicine*, **40**, 37S-61S.
- [15] International Commission on Radiological Protection (ICRP) (1991) 1990 Recommendations of the International Commission of Radiological Protection. ICRP Publication 60. Pergamon Press, New York.
- [16] Fleischmann, A., Waser, B. and Reubi, J.C. (2007) Overexpression of Gastrin-Releasing Peptide Receptors in Tumor-Associated Blood Vessels of Human Ovarian Neoplasms. *Cellular Oncology*, **29**, 421-433.
- [17] Sharif, T.R., Luo, W. and Sharif, M. (1997) Functional Expression of Bombesin Receptor in Most Adult and Pediatric Human Glioblastoma Cell Lines: Role in Mitogenesis and in Stimulating the Mitogen-Activated Protein Kinase Pathway. *Molecular and Cellular Endocrinology*, **130**, 119-130. [https://doi.org/10.1016/S0303-7207\(97\)00080-4](https://doi.org/10.1016/S0303-7207(97)00080-4)
- [18] Chen, X., Park, R., Hou, Y., *et al.* (2004) microPET and Autoradiographic Imaging of GRP Receptor Expression with  $^{64}\text{Cu}$ -DOTA-[Lys<sup>3</sup>] Bombesin in Human Prostate Adenocarcinoma Xenografts. *Journal of Nuclear Medicine*, **45**, 1390-1397.
- [19] Zhang, X., Cai, W., Cao, F., *et al.* (2006)  $^{18}\text{F}$ -Labeled Bombesin Analogs for Targeting GRP Receptor-Expressing Prostate Cancer. *Journal of Nuclear Medicine*, **47**, 492-501.
- [20] Smith, C.J., Volkert, W.A. and Hoffman, T.J. (2005) Radiolabeled Peptide Conjugates for Targeting of the Bombesin Receptor Superfamily Subtypes. *Nuclear Medi-*

- cine and Biology*, **32**, 733-740. <https://doi.org/10.1016/j.nucmedbio.2005.05.005>
- [21] Prasanphanich, A.F., Nanda, P.K., Rold, T.L., *et al.* (2007) [<sup>64</sup>Cu-NOTA-8-Aoc-BBN-(7-14) NH<sub>2</sub>] Targeting Vector for Positron-Emission Tomography Imaging of Gastrin-Releasing Peptide Receptor-Expressing Tissues. *Proceedings of the National Academy of Sciences of the United States of America*, **104**, 12462-12467. <https://doi.org/10.1073/pnas.0705347104>
- [22] Liu, Z., Niu, G., Wang, F. and Chen, X. (2009) <sup>68</sup>Ga-Labeled NOTA-RGD-BBN Peptide for Dual Integrin and GRPR-Targeted Tumor Imaging. *European Journal of Nuclear Medicine and Molecular Imaging*, **36**, 1483-1494. <https://doi.org/10.1007/s00259-009-1123-z>
- [23] Gonzalez, N., Moody, T.W., Igarashi, H., Ito, T. and Jensen, R.T. (2008) Bombesin-Related Peptides and Their Receptors: Recent Advances in Their Role in Physiology and Disease States. *Current Opinion in Endocrinology, Diabetes and Obesity*, **15**, 58-64. <https://doi.org/10.1097/MED.0b013e3282f3709b>
- [24] Strauss, L.G., Koczan, D., Seiz, M., *et al.* (2012) Correlation of the Ga-68-Bombesin analog Ga-68-BZH3 with Receptors Expression in Gliomas as Measured by Quantitative Dynamic Positron Emission Tomography (dPET) and Gene Arrays. *Molecular Imaging and Biology*, **14**, 376-383. <https://doi.org/10.1007/s11307-011-0508-0>
- [25] Mansi, R., Minamimoto, R., Mäcke, H., *et al.* (2016) Bombesin-Targeted PET of Prostate Cancer. *The Journal of Nuclear Medicine*, **57**, 67S-72S. <https://doi.org/10.2967/jnumed.115.170977>
- [26] Schroeder, R.P.J., de Visser, M., van Weerden, W.M., de Ridder, C.M.A., Reneman, S., Melis, M., Breeman, W.A.P., Krenning, E.P. and de Jong, M. (2010) Androgen-Regulated Gastrin-Releasing Peptide Receptor Expression in Androgen-Dependent Human Prostate Tumor Xenografts. *International Journal of Cancer*, **126**, 2826-2834. <https://doi.org/10.1002/ijc.25000>
- [27] Ramos-Álvarez, I., Moreno, P., Mantey, S.A., Nakamura, T., Nuche-Berenguer, B., Moody, T.W., Coy, D.H. and Jensen, R.T. (2015) Insights into Bombesin Receptors and Ligands: Highlighting Recent Advances. *Peptides*, **72**, 128-144. <https://doi.org/10.1016/j.peptides.2015.04.026>